Local Composition of Nanophase-Separated Mixed Polymer Brushes

Svetlana Santer,*,† Alexey Kopyshev, Hyun-Kwan Yang, and Jürgen Rühe

Department of Microsystems Engineering (IMTEK), University of Freiburg, Georges-Koehler-Allee 103, D-79110 Freiburg, Germany

Received January 13, 2006; Revised Manuscript Received February 28, 2006

ABSTRACT: Polystyrene−poly(methyl methacrylate) (PS−PMMA) mixed brushes synthesized by surface-initiated polymerization show nanophase separation into defined pattern depending on the molecular parameters of the brushes. Two sets of mixed brushes are studied: (i) with fixed grafting density and molecular weight of the PS chains, but differing in the molecular weight of PMMA polymer, and (ii) with varying grafting density of the PMMA chains while that of the PS chains and the molecular weight of PS and PMMA chains are kept constant. The local distribution of PS and PMMA chains within the monolayer and the size, shape, and position of the domains constituting the nanopattern are found to vary with the nature of the solvent to which the brushes are exposed. The brushes are treated cyclically first with either a good solvent for both blocks, leading to strong swelling and structure erasure, and then with a selective solvent, which induces the nanophase separation. It was found that in the case of the brush exposed to toluene solvent (good solvent for both polymers) the brush surface exhibiting a small variation in topography has a heterogeneous surface composition, with the nanoscopic areas having only PS or PMMA chains at the surface. When the brush is treated with acetone solvent, which is better for the PMMA chains, the surface consists only of PMMA chains, and the topography assumes a more pronounced relief. We introduce the concept of the local domain memory effect of the brushes, i.e., whether the brush locally forms always the same pattern or if the local assembly of the domains emerges in different places every time the transition to the structured state occurs.

Introduction

The interest in polymer brushes has progressively grown from the development of theoretical concepts[1−6] to the realization of experimental systems and the emergence of novel applications.[7−10] Especially the latter has evolved strongly along with the development of a polymerization procedure where the polymer molecules are grown directly on a surface in situ.[11] A variety of growth strategies allows adjustment of molecular parameters and composition of the brushes in a controlled way. Of special interest are systems in which two different types of polymer molecules are attached to one surface. ATRP is typically used for the synthesis of diblock copolymer brushes with a variation of brush composition along the chains,[12−16] while free radical polymerization is frequently applied for the synthesis of mixed brushes in which two types of (homo-)polymer chains are attached at random positions on the surface.[17−23] Both systems lead to microphase-separated structures if two incompatible polymers are used. For the characterization of both diblock copolymer and mixed brushes, the main effort so far mostly has been put on identifying the different topographies and subsequently measuring the contact angles of water on the surface of the brushes.[24−26] These investigations have been fostered by certain key applications, such as designing surfaces with switchable wettability and adhesion properties. It was observed that contact with different solvents can influence the surface topography significantly. Exposure to selective and nonselective solvents allows to switch the topography of the samples on a nanoscale, rendering polymer brushes interesting for nanotechnology.

Recently, we have introduced a new method to move nano-objects on a polymer surface consisting of diblock copolymer and mixed brushes.[27,28] The brushes consist of two polymeric components, A and B, which are incompatible with each other and show microphase separation into patterns of defined size and shape.[8−26,29−32] As the domains in such systems are typically only on the scale of a few nanometers and do not change even upon prolonged annealing, one might call such systems "nanophase separated". The size and shape of the domains depend not only on molecular parameters of the brushes, such as grafting density, molecular weight of the chains, and the mass ratio of A to B polymer, but also on the selectivity of the solvent to which the brush was exposed. In the case of mixed brushes it was shown theoretically[19,29,32−34] and experimentally[19] that in a nonselective solvent the A and B polymers segregate laterally into so-called "ripple structure", while upon exposure to a selective solvent, a transition to a layered ("dimple") structure, in which the unfavored component forms clusters, occurs. This transition results in significant changes of the brush topography.

We have shown that the same area on the brush can be turned into different topographical states, namely nanostructured and flat,[27,28] through subsequent exposure of the sample to different solvents. One of the solvents is selective for a certain chain and the other is a nonselective, i.e., good solvent for both A and B components. Changes of the topography are accompanied by the redistribution of the chains A and B on the topmost surface of the brush. On a macroscopic scale this results in a change of the hydrophobicity/hydrophilicity of the samples, which causes a change of the wetting behavior of the surfaces. Experimentally this behavior has been reported for a variety of tri- and diblock copolymers[16,35−38] and mixed brushes.[17−24] On the nanoscale, the topography fluctuations determine a spatial variation of the surface energy on the length scale of the domain size. This results in dynamically fluctuating force fields acting on objects located on the polymer surface. Such fluctuating force fields can be used as a driving force for the movement of adsorbed nanoparticles.[27,28]

† Born Prokhorova.

* To whom any correspondence should be addressed. E-mail: ssanter@imtek.de.

10.1021/ma060092y CCC: $33.50
Published on Web 03/23/2006

Scheme 1. Chemical Structure of PS−PMMA Mixed Brush

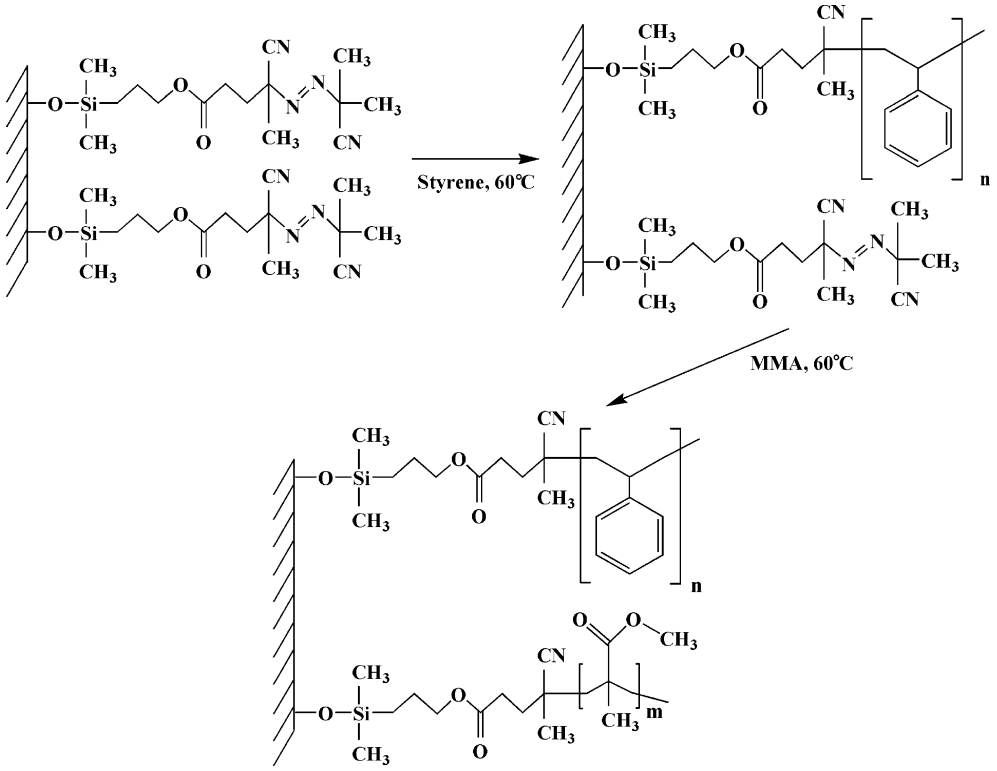

Table 1. Molecular Parameters of PS−PMMA Mixed Brushes

	M_n^{PS} [a] [g/mol]	$\Gamma^{PS}(t)$ [μmol/m^2]	σ^{PS} [nm^{-2}]	h^{PS} [b] [nm]	M_n^{PMMA} [a] [g/mol]	$\Gamma^{total}(t)$ [μmol/m^2]	σ^{total} [nm^{-2}]	h^{total} [nm]	h^{PMMA} [b] [nm]
I	3×10^5	0.071	0.042	20	0.3×10^6	0.100	0.060	25	5
II	3×10^5	0.071	0.042	20	0.5×10^6	0.100	0.060	30	10
III	3×10^5	0.071	0.042	20	1×10^6	0.100	0.060	34	14
IV	3×10^5	0.071	0.042	20	1×10^6	0.093	0.056	30	10
V	3×10^5	0.071	0.042	20	1×10^6	0.115	0.069	40	20
VI	3×10^5	0.071	0.042	20	1×10^6	0.124	0.075	50	30

[a] The number-average molecular weights of the free PS and PMMA polymers were measured using an Agilent GPC setup. [b] h^{PMMA} was calculated as the difference of the total dry thickness and the thickness of the PS brushes: $h^{PMMA} = h^{total} - h^{PS}$.

In this paper, we investigate PS−PMMA mixed brushes that can be divided into two sets: one series consists of brushes with fixed grafting density and fixed molecular weight of the polystyrene chains and varying molecular weight of the second, the poly(methyl methacrylate) (PMMA) chains; the second set comprises brushes of varying grafting density of PMMA while the molecular weight of the PS and PMMA chains and the grafting density of the PS chains are kept constant. For these two classes, we investigate the structure of the nanopatterns and how they depend on the solvent exposure. In addition, we address the question of what the influence of the nature of the solvent and the drying conditions have on the nanopattern at the single domain level. We observe and track the shape, size, and location of single domains in the nanopattern during and after exposure to varying environmental conditions.

Materials and Methods

Synthesis of PS−PMMA Mixed Brushes. The synthesis of PS−PMMA mixed brushes was carried out as described elsewhere.[39] Here we report without details the main steps of the synthesis. The dimethylchlorosilylpropyl 4-isobutyronitrile-4-cyanopentanoate (AMCS) initiator was prepared as described in ref 40. The azo initiator was immobilized on the surface of a silicon crystal in the presence of triethylamine (TEA) in dry toluene solution under a nitrogen atmosphere. An excess of initiator was used to perform a condensation reaction between the chlorosilane groups and the silanol groups on the surface.[40−43] This reaction results in a well-defined monolayer, covalently attached to the silicon surface (Scheme 1). The roughness of the surface covered with the initiator is 0.4 nm as determined from atomic force microscopy (AFM) and X-ray reflectometry (XRR) measurements. This value is the same as that of the roughness of the blank silicon wafer. The grafting density of the initiator molecules is typically around 1.8 μmol/m^2, which corresponds to 1.08 nm^{-2}.[40−43]

The surface-initiated radical polymerization of styrene and (methyl methacrylate) was carried out through thermal initiation at 60 °C. In the first step the polystyrene (PS) homopolymer was grown from the initiator surface. For all brushes discussed here, the polymerization time for the PS chains was 3 h, and the concentration of the styrene monomer in toluene was 1:1 (v/v). These reaction conditions yield a molecular weight of the PS chains of $M_n = 3 \times 10^5$ g/mol and a grafting density of $\Gamma(t) = 0.071$ μmol/m^2, i.e., $\sigma = 0.042$ nm^{-2} (Table 1).[41,42] After polymerization of the PS homopolymer, the samples were extracted with cold toluene in an externally cooled Soxhlet apparatus for at least 10 h. This allows to remove all not covalently attached polymers chains formed in solution.[40−43] The dry thickness of the brush was 20 ± 1 nm as determined from ellipsometry, XRR, and AFM measurements. After polymerization, the silicon wafer containing the PS brush was cut into several pieces, which were used for growing a second homopolymer. Thus, a series of mixed brushes were synthesized having identical molecular characteristics (molecular

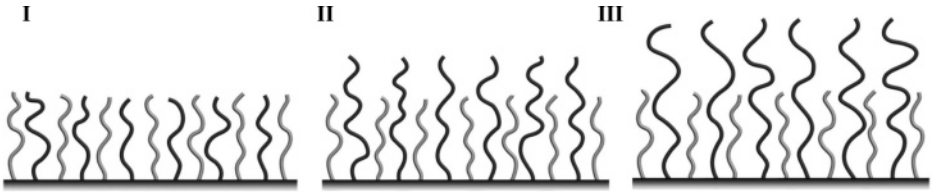

Figure 1. Simplified scheme of the PS−PMMA mixed brushes having the same molecular weight and grafting density of the PS chains (gray) and similar total grafting density and different molecular weight of PMMA chains (black).

weight and grafting density) of the PS chains and different characteristics of the second homopolymer (PMMA).

The growth of the second polymer was initiated from the initiator, which was not activated during the first reaction (Scheme 1). By varying the polymerization time at constant MMA/toluene concentration (in this paper 1:1 v/v), mixed brushes with different grafting density of PMMA were synthesized (Table 1). When the polymerization time of PMMA is increased from 1 to 2 h and then to 2.5 h, the overall grafting density of the brushes (Table 1) increases from $\Gamma(t) = 0.093$ μmol/m^2 ($\sigma = 0.056$ nm^{-2}) to $\Gamma(t) = 0.115$ μmol/m^2 ($\sigma = 0.069$ nm^{-2}), and $\Gamma(t) = 0.124$ μmol/m^2 ($\sigma = 0.075$ nm^{-2}), respectively.[43] When the polymerization time of the PMMA homopolymer is kept constant ($\Gamma(t) = 0.1$ μmol/m^2 ($\sigma = 0.06$ nm^{-2})), the molecular mass of the PMMA homopolymer is changed by varying the MMA/toluene concentration (Table 1, brushes I, II, III).[43] After synthesis of the second polymer, the samples were again extracted with toluene to remove unbound PMMA chains.

Instrumentation. An atomic force microscope (AFM) (MultiMode, Veeco Metrology Group) was used to characterize the morphology of the layers. Tapping mode images were acquired using silicon cantilevers (Olympus) with a resonance frequency of ~300 kHz, a spring constant of ~50 N/m, and a tip radius of ~10 nm. For filling the measurement cell with solvents or vapors we built a system with a mechanical pump that connects reservoirs filled with either dichloromethane, acetone, acetic acid, and toluene solvents and their vapors. With a corresponding switch it was possible to control the flow of the different vapors into the measurement cell within several seconds and switch between different vapors and air. After the sample was exposed to the chosen vapor or solvent, air was pumped through the cell for 2 min in order to dry the sample. AFM images were recorded in air at a relative humidity of 40−45% and at room temperature (~25 °C). Commercial software (Nanoscope IIIa, DI) was used for the image analysis on several areas of (5 μm)^2 and (2 μm)^2 in size and averaged over 20 micrographs. The roughness of the surfaces in terms of the root-mean-square deviation from the mean plane (rms) was calculated taking into account an area of (2 μm)^2.

The thickness of the mixed brushes was characterized using a commercial DRE-XO2 C ellipsometer operating with a 638.2 nm He/Ne laser at an incident angle of 70°. The refractive index of PMMA was taken as $n = 1.49$, while the refractive index of the mixed layer (PMMA and PS) was varied according to the composition. Results were obtained from three different spots on each wafer with three measurements per spot. The characterization of the brushes was also carried out using a 1.6 kW X-ray reflectometer from Bruker AXS (Cu Kα, $\lambda = 0.154$ nm) (Siemens/Bruker D5000).

Results and Discussion

Series I: Variation of the Molecular Weight of the PMMA Chains at Constant Grafting Density. For the first series of mixed brushes studied here the grafting density of the chains was $\Gamma(t) = 0.1$ μmol/m^2 ($\sigma = 0.06$ nm^{-2}); i.e., the distance d between two neighboring chains was around 4.08 nm ($d = 1/\sqrt{\sigma}$). As during the growth of the PMMA chains different monomer concentration were employed, the molecular weight of the surface-attached chains and the ratio ϕ between the total number of PS segments to total number of PMMA segments varied accordingly (Table 1). When the grafting density of the two chains is similar, ϕ can be calculated as the ratio of the PMMA and PS molecular weights: $\phi = M_n^{PMMA}/M_n^{PS}$. In the samples studied here it varies from $\phi = 1$ to $\phi = 3.3$. A schematic representation of the brushes is shown in Figure 1.

It is known that binary brushes consisting of incompatible polymers show microphase separation on a nanometer length scale into different patterns, depending on molecular parameters and on external conditions such as the type of solvent to which the brush is exposed.[17−24] To understand how different solvents influence the morphology of a certain brush, we first used toluene and acetone as typical examples. Acetone is a better solvent for PMMA than for PS, while toluene is a good one for both polymers but slightly favors PS over PMMA.[44] The topography of the brushes was examined by tapping mode AFM measurements after exposure to each solvent.

After installing the samples into the AFM, they were treated with acetone by pumping the solvent through the cell for 10 s, followed by drying in an air flow for 2 min. The topography in all three cases is not smooth but has a roughness of 8.5 nm (Figure 2a−c). The formed patterns are homogeneous in size with heights of 20, 25, and 27 nm for the brushes I, II, and III, respectively. The average distance between the pattern is around 120 nm. The shape of the brush pattern can be best described as a "dimple-like" structure. The advancing contact angle of water of all three brushes is 73 ± 1°, which corresponds to the advancing contact angle of water on a flat PMMA surface.

Without changing the scanning position on the brush, toluene was pumped through the liquid cell for 10 s, and the samples were dried in air for 2 min. The topography of the brushes recorded at the very same place is shown in Figure 2d−f. The precise identification of a specific location is accomplished by choosing suitable reference points; these are small defects found near the edge in the lower right part of the micrographs. After treatment with toluene (better solvent for the PS polymer), the topography of the brushes became smoother, and the rms roughness dropped to 1.5 nm for all three brushes. The height of the pattern formed is 4 ± 1 nm for brushes I and II and 5 ± 2 nm for brush III (Table 2).

The phase AFM micrographs of the same areas are shown in Figure 2g−i. The images were recorded in the moderate tapping mode, in which the phase contrast between different areas on the micrographs is caused by differences in material stiffness.[45] For the measurement setup used here, a higher stiffness causes a larger phase shift (at moderate tapping mode ($r_{sp} \sim 0.7$)), which is represented by a brighter color in the micrographs. As the Young modulus of PMMA is higher than that of PS, brighter locations can be attributed to higher PMMA contents. The phase images of the three samples reveal a pronounced binary distribution with phase contrast of 30° for all brushes. There is a direct connection between the topography (Figure 2d−f) and phase pattern (Figure 2g−i): the "folds" visible in Figure 2d−f

Table 2. Size of the Topography Patterns for PS−PMMA Mixed Brushes after Solvent Treatment As Measured by AFM

	film thickness	acetone		toluene	
	h,[a] nm	*H*,[b] nm	*d*,[c] nm	*H*,[b] nm	*d*,[c] nm
I	25	20 ± 2	∼120	4 ± 1	∼200
II	30	25 ± 3	∼120	4 ± 1	∼200
III	34	27 ± 3	∼120	5 ± 2	∼200
IV	30	25 ± 3	∼120	4 ± 1	∼200
V	40	30 ± 3	∼150	4 ± 2	∼200
VI	50	10 ± 3	∼120	6 ± 2	∼200

[a] *h* is the total dry thickness of the brush (Table 1). [b] *H* is the height of the patterns of PS−PMMA mixed brushes. [c] *d* is the average distance between the centers of two neighboring brush patterns.

correspond to the bright areas on the phase images. The coverage of bright areas on the phase images increases from 30% for brush I to 37% for brush II and 45% for brush III. Remarkably, this coincides with the total amount of PMMA polymer within the brushes (32%, 40%, and 45% for brushes I, II, and III, respectively). It should be mentioned that, after treatment with acetone, no phase contrast was obtained on the same areas (see Supporting Information).

Series II: Variation of the Grafting Density. In the second set of samples (Table 1), the ratio of PMMA/PS is changed as the grafting density of the PMMA is varied, while the molecular weight of the polymers is kept constant (Figure 3). In these samples the brush topography after acetone treatment shows features similar to the first set (Figure 4a−c).

The roughness (rms) of the surfaces is 8.5 nm, and the phase micrographs after treatment with acetone show no contrast, as in the case of the first set of brushes. The height of the pattern increases from 25 ± 3 nm for brush IV to 30 ± 3 nm for brush V (Figure 4a,b, respectively). Brush VI, which has the highest total dry thickness (50 nm) (Table 2), microphase-separates into a semispherical pattern with height 10 ± 3 nm (Figure 4c). As in the investigations of the first series, we used areas that can be tracked with the help of characteristic defects; e.g., for brush V we chose a characteristic bright spot in the upper left edge (Figure 4b).

After treatment with toluene, the topography became smooth, with a roughness of 1.5 nm. The height of the features for brushes IV and V is 4 ± 1 nm, while the depth of the "holes"

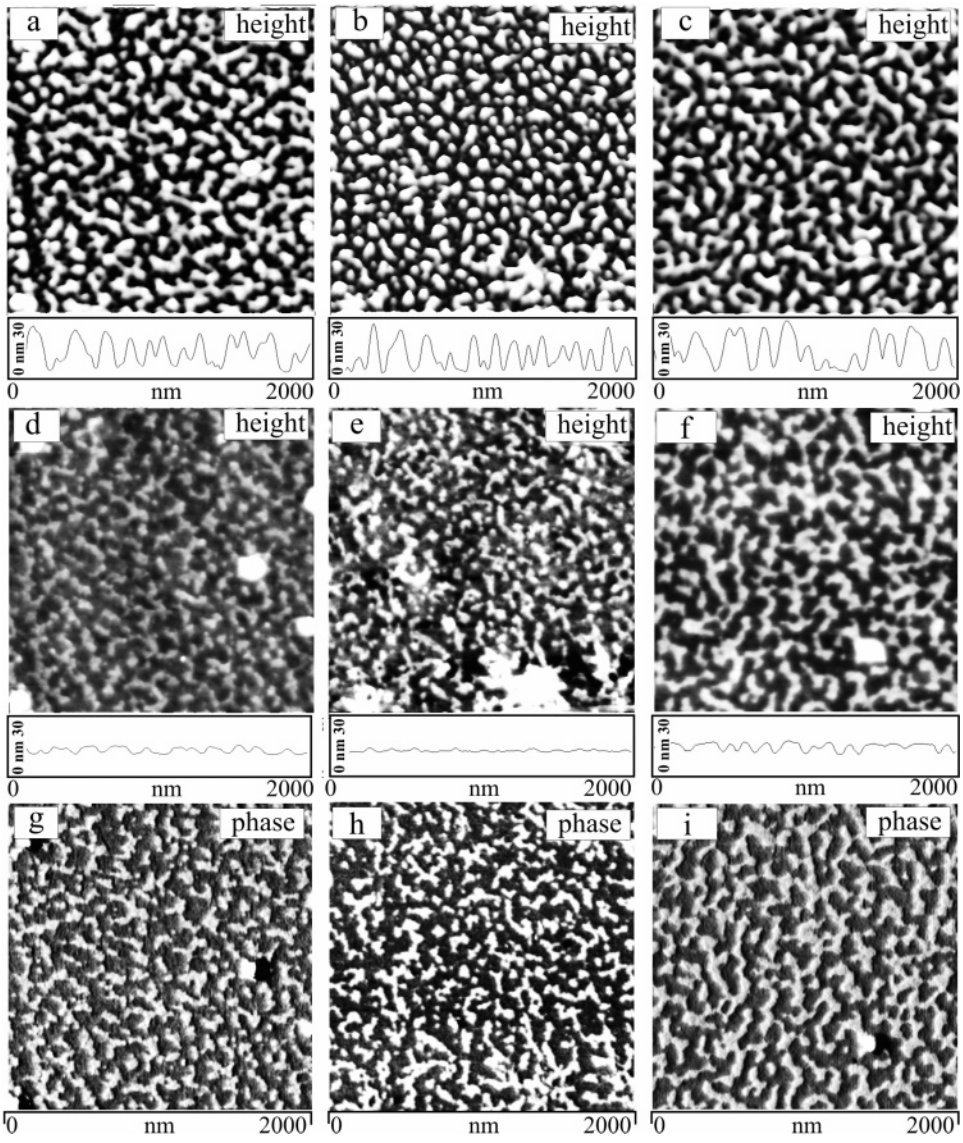

Figure 2. AFM micrographs of the three brushes I (a, d, g), II (b, e, h), and III (c, f, i) (Table 1), sharing similar grafting density but differing in the ratio $\phi = M_n^{PMMA}/M_n^{PS}$ (PS molecular weight is fixed) as 1, 1.7, and 3.3, respectively. (a, b, c) show the topography of the brushes after treatment with acetone and their cross section taken at an arbitrary line. (d, e, f) After exposure of the samples to toluene, the topography was recorded at the same areas as in (a, b, c). (g, h, i) show the phase images (vertical scale, 30°) of the areas from (d, e, f).

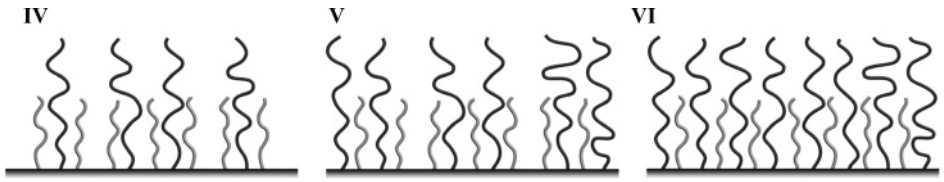

Figure 3. Simplified scheme of the PS−PMMA mixed brushes (series II) having the same molecular weight of PS (gray) and PMMA (black) chains and differing in grafting density of PMMA chains.

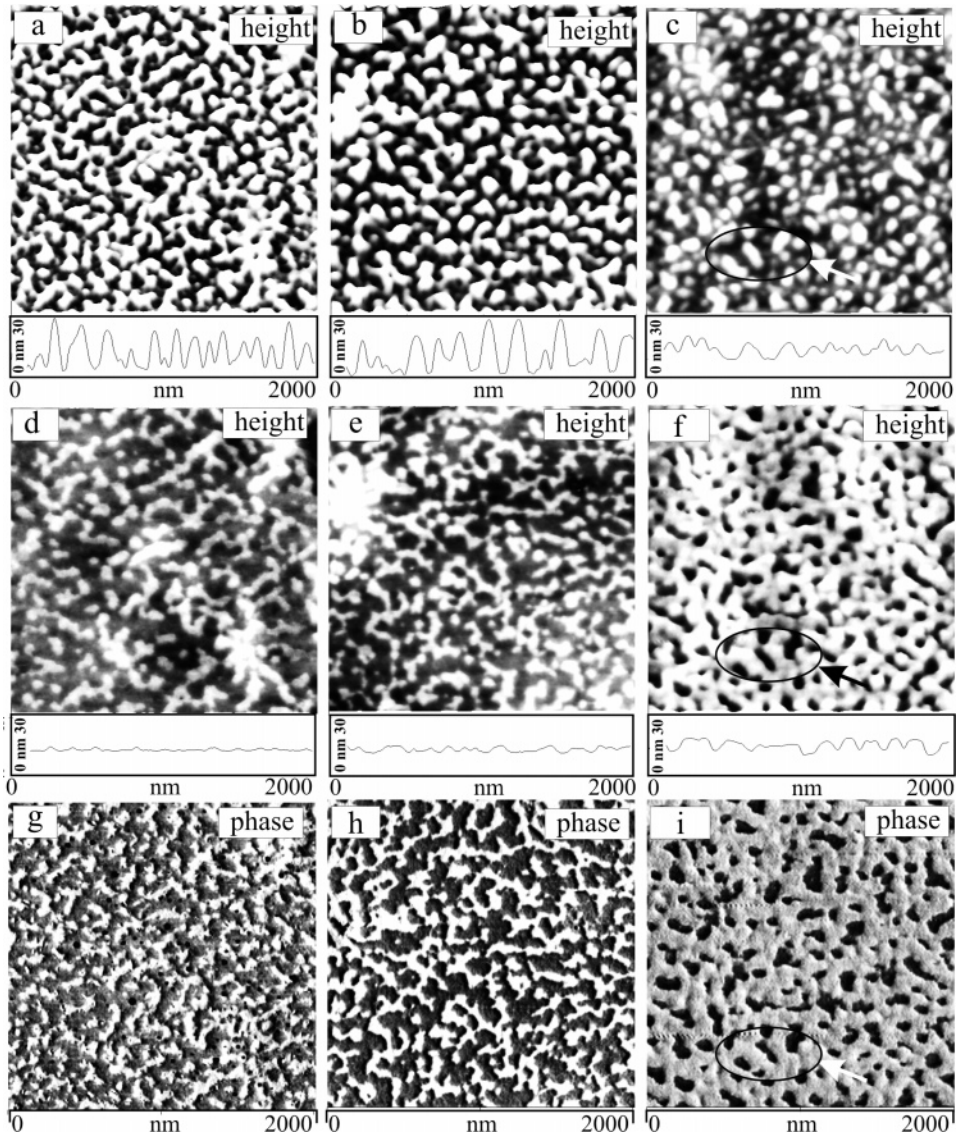

Figure 4. AFM micrographs of the second set of brushes IV, V, and VI (Table 1) with constant molecular weight of PS ($M_n = 3 \times 10^5$ g/mol) and PMMA ($M_n = 1 \times 10^6$ g/mol) but increasing PMMA grafting density (σ(a) < σ(b) < σ(c)). After exposure to acetone (a, b, c), the brush topography exhibits dimplelike (a, b) or semispherical (c) patterns. (d, e, f) show the same area after treatment with toluene (better solvent for the PS). Phase micrographs of the areas in (g, h, i) reveal a pronounced contrast between the depressions and the patterns (vertical scale: 30°).

in brush VI is 8 ± 2 nm. The average distance between the patterns formed (ripples or holes) for all three brushes is the same, i.e., ~200 nm (Table 2). The phase micrographs of the brushes after toluene exposure (Figure 4 g−i) show a pronounced distribution of two different phases. As in the case of the first set of brushes, the dark areas correspond to the regions of lower height on the height images. The bright areas correspond to regions with higher phase shift. Remarkably, in the case of brush VI, there is an inversion of patterns between the two states (after treatment with acetone and toluene). Indeed, when just searching for the three "micelles" marked by an oval in Figure 4c, they turned into three "holes" (Figure 4f, marked by the black oval) after toluene exposure and appeared as the areas with the smaller phase shift in the phase micrographs (Figure 4i). This behavior is common for all patterns of brush VI.

The area with the higher phase shift increases with grafting density, from 35% for the brush IV to 60% for the brush V and 80% for the brush VI (Table 1). The fraction of the area with high phase shift coincides with the mass fraction of PMMA in the brushes, which is 31%, 62%, and 75% for brush IV, V, and VI, respectively. This compares well to series I, where the mass fraction of PMMA also varies, caused by the increase of the molecular weight of the PMMA chains.

Vapor Experiments. In all experiments described so far solvent exposure followed by a drying process was employed. The drying process of surface-attached layers, however, is rather complicated. To prove that the observed structures are not caused by artifacts of the drying process, similar experiments were carried out in vapor. As an example, we discuss the morphology of one of the brushes (brush IV, Figure 5a,b) in toluene vapor. The height image reveals a smooth topography with a roughness of 0.7 nm, while the phase micrograph shows a pronounced heterogeneous surface, with regions of high phase contrast (bright areas) and low phase contrast (dark "ripples"). When the sample is exposed to solvent vapor, the phase transition can be almost followed in real time. In the case of brush V, the in-situ switching of the brush topography from the dry state (after toluene treatment) to a swollen one was carried out by pumping saturated toluene vapor into the cell during image acquisition. The moment when the solvent vapor was introduced can be easily identified by a disturbance of the image recording, marked by an arrow in the figure. The scanning direction was from top to bottom (Figure 5c,d). After introduction of the vapor, a short instability of the AFM imaging process was observed. During this time the cantilever moved by about 120 nm[46] in the scanning direction. As the image acquisition frequency was 2 Hz, corresponding to a scanning speed along the slow scan direction of 19.5 nm/s, the time required for switching from the dry to the swollen topography can be estimated from the image to be 6 s.

The zone of instability in the image acquisition process during solvent vapor introduction is due to the sum of two very different effects: on one hand, since the ambient conditions are changed, the dynamic parameters of the tip (oscillation frequency, amplitude, quality factor) change as well. This is because many processes are taking place at the same time when the vapor is pumped into the area between the scanning AFM tip and the polymer surface: (i) change of the refractive index of the surrounding medium through which the laser beam passes, (ii) local changes in total pressure, (iii) condensation of vapor on the AFM cantilever, and (iv) hydrodynamic influences of the vapor flow on the cantilever oscillation. On the other hand, swelling or reorganization of the polymer structure itself starts immediately after vapor introduction. This process may induce height perturbations during the scanning of the AFM cantilever. In general, both effects may occur over a broad range of time scales, such that a precise analysis cannot easily be made. Thus, we can only conclude that the swelling appears either on the same or a smaller time scale as the duration of the instability observed during the AFM experiment.

We briefly summarize our findings up to this point. After toluene treatment, the AFM micrographs show a phase contrast, indicating a heterogeneous distribution of PS and PMMA chains at the brush surface. In the phase images, the coverage with bright areas increases with increasing amount of the PMMA present (due to either increased grafting density or increased molecular weight), suggesting a corresponding increase of PMMA at the topmost layers of the polymer brush. After treatment with acetone, on the other hand, there is no noticeable phase contrast, and one expects only PMMA to be present at the brush surface. These assumptions are also supported by contact angle measurements. Our results suggest that one may always identify the bright areas in the phase images with PMMA. This will be confirmed in the following section.

Domain Memory. So far, the experimental results show that we are able to *locally* study the brush composition over many cycles of topography switching. An interesting question now is whether the domains emerge at completely random positions or whether there is a certain persistence of position and shape of domains during erasure and regeneration.

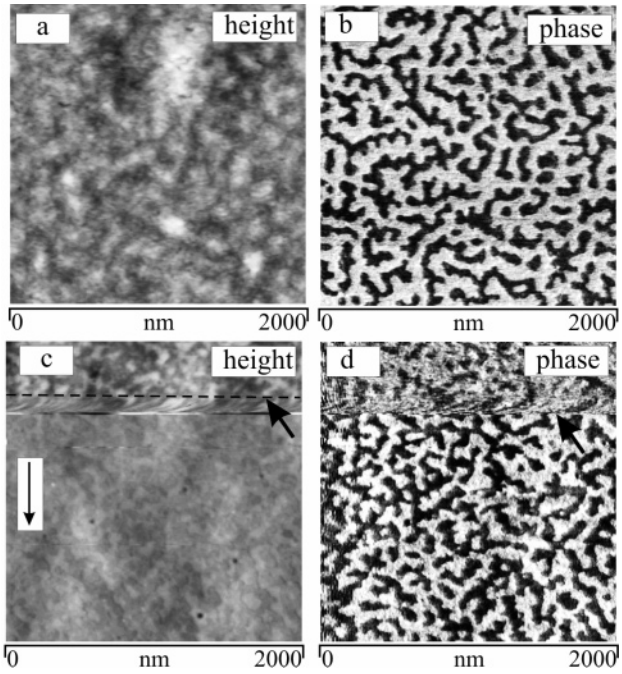

Figure 5. Height and phase AFM micrographs of the brushes IV (a, b) and V (c, d) acquired after toluene vapor exposure. The topography is smooth, while the phase images reveals a heterogeneous distribution of the two components, inducing high phase shift (bright areas) and low phase shift (dark areas). (c, d) During scanning from top to bottom, toluene vapor is pumped into the liquid cell at the scan position indicated by the bold arrow. After a short instability time at which the distance $l = 120$ nm is scanned ($\sim$6 s), the topography of the brush V became smoother. The imaging was carried out using the moderate tapping mode ($r_{sp} \sim 0.7$) with the driving amplitude of $A_0 = 70$ nm.

To illustrate this question, we take brush II as an example, a selected area of which was scanned after treatment with acetone and toluene (Figure 6). To have a good position reference point, we scratched the surface mechanically. This results in a 400 nm wide stripe extending from the upper right corner to the lower left corner of the image (Figure 6), where the film is largely removed and only bare silicon is left behind. After treatment with acetone, the stripe was empty. However, after exposure to toluene, a fraction of the polymer adsorbed on the stripe's surface, filling it almost completely with a 1 nm thick polymer layer (Figures 6c,d,d1,d2). Phase images reveal that the material adsorbed to the stripe has a higher phase shift (Figures 6d,d1,d2). It is well-known that PMMA preferentially adsorbs to silicon surface. This agrees well with the finding described above that the bright areas in the phase images consist of PMMA chains. After exposure of the same area to acetone, the chains receded from the stripe (Figures 6a,b,b1,b2). Reexposure to toluene solvent leads to readsorption of the polymer to the surface of the stripe (Figure 6d2). Although a width of 400 nm seems a lot for coverage by simply "leaning over" of polymer chains, it should be noted that the dry layer thickness is around 30 nm. Thus, half of the channel width is only roughly 7 times larger than the layer thickness. For comparison the contour length of a 1×10^6 g/mol PMMA chain can be estimated to be roughly 2.5 μm.

In tracing the local structure over repeated solvent switching cycles, one finds that characteristic patterns persist at the very same places (Figure 7). In the series of the micrographs in Figure 7, a certain area on the brush was selected, and the topography

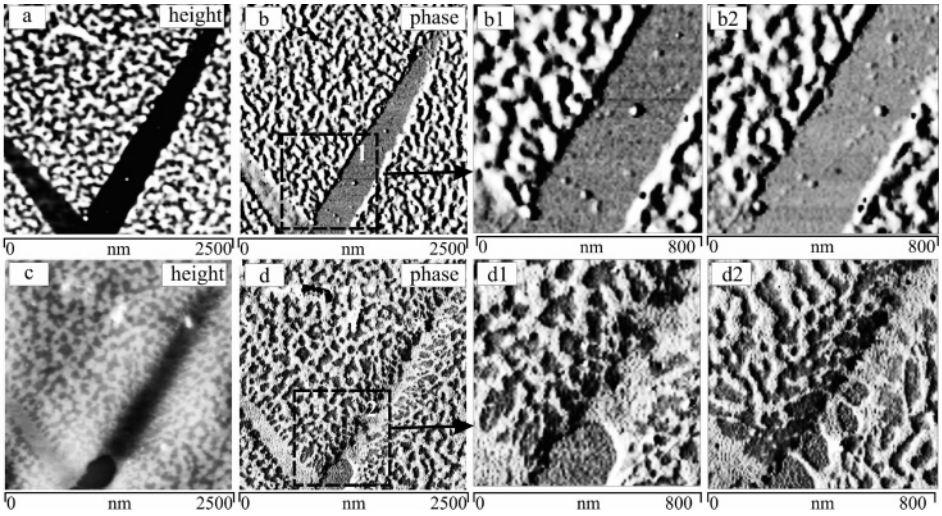

Figure 6. AFM micrographs of the brush II after acetone exposure (a, b) and toluene treatment (c, d). The brush was scratched that results to the stripe of bear silicon surface going across the image from the right upper to the left bottom corner. The phase image in (b) has no significant contrast, while the one in (d) shows two-phase map of the surface. The micrographs b1, b2, d1, and d2 demonstrate details of the selected area marked by dashed black square. After treatment with acetone (b1), the same area was exposed to toluene (d1), again reexposed to acetone (b2) followed by treatment with toluene (d2).

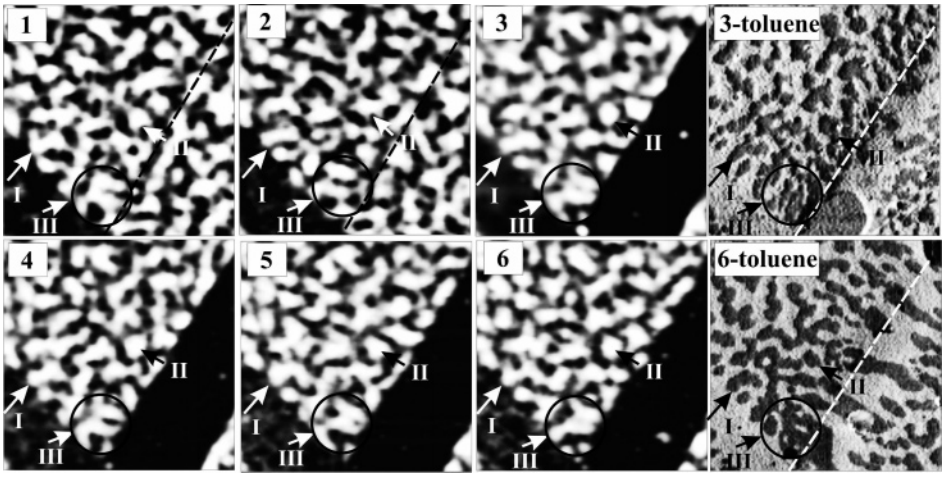

Figure 7. Height AFM micrographs of the topography of brush II recorded after exposure to acetone. The images were acquired after six subsequent switching of the solvent from acetone to toluene and back to acetone. The size of the micrographs is 900 nm × 900 nm. 3-Toluene and 6-toluene are the same areas after treatment with toluene in the 3rd and 6th cycles, respectively. I, II, and III indicate the domains discussed in the text.

was recorded after each of nine cycles of acetone−toluene treatment (see movie in Supporting Information). Micrographs 1 and 2 show the same area as in the images 3, 4, 5, and 6, but before scratching. The dashed black line in Figures 7, 1 and 2 indicate the edge where the brush was removed. The marked domains (I, II, and III) appear after each cycle of topography switching at the very same position with a slight variation in overall shape. The variation of domain shape during topography switching is different for each domain: some of them are strongly persistent (domains I and II) and others (domain III) possess a weaker memory, but in all cases there appear to be pronounced "nucleation centers" that pin domain formation during nanophase separation.

Influence of Solvents. An important question is whether the observations of domain memory are solely due to a specific solvent combination (toluene/acetone) or whether other good or selective solvents can be used. In addition, it is of interest which of the polymer is located where in the brush: the difference in solvent quality for the two polymers determines the extent of phase separation, while the better soluble polymer is more likely to be located in the upper layer of the brush. The brushes were treated with four different solvents: acetone, toluene, acetic acid, and dichloromethane. According to the data in ref 44, dichloromethane and toluene are good solvents for both polymers while acetone and acetic acid both favor PMMA.

We illustrate our findings using brush IV as an example, which is characterized by a total dry thickness of 30 nm (Tables 1 and 2) and a total grafting density of $\Gamma(t) = 0.093\ \mu\text{mol/m}^2$ ($\sigma = 0.056\ \text{nm}^{-2}$, $d = 4.22$ nm). The topography of the brush after exposure to each of the solvents was recorded at the same location. This area can be identified from the three characteristic features on the brush marked by the arrows in Figure 8a−d. When searching for single patterns, we have selected an area marked by a dashed black square, the enlargements of which are placed to the right of each original micrograph (Figure 8). On an area of 600 nm × 500 nm, among others, a characteristic Π-shaped pattern can be recognized (for clarity, we marked the pattern with a dashed line).

After treatment with acetone (Figure 8a), the Π-shaped pattern appeared as a depression with a depth of 25 nm and a width of 80 nm. Accordingly, in the phase image this feature cannot be clearly recognized as the phase contrast is only very weak. After toluene exposure (slightly better solvent for PS) the Π pattern appeared as a protrusion with a height of 4 nm and a width of

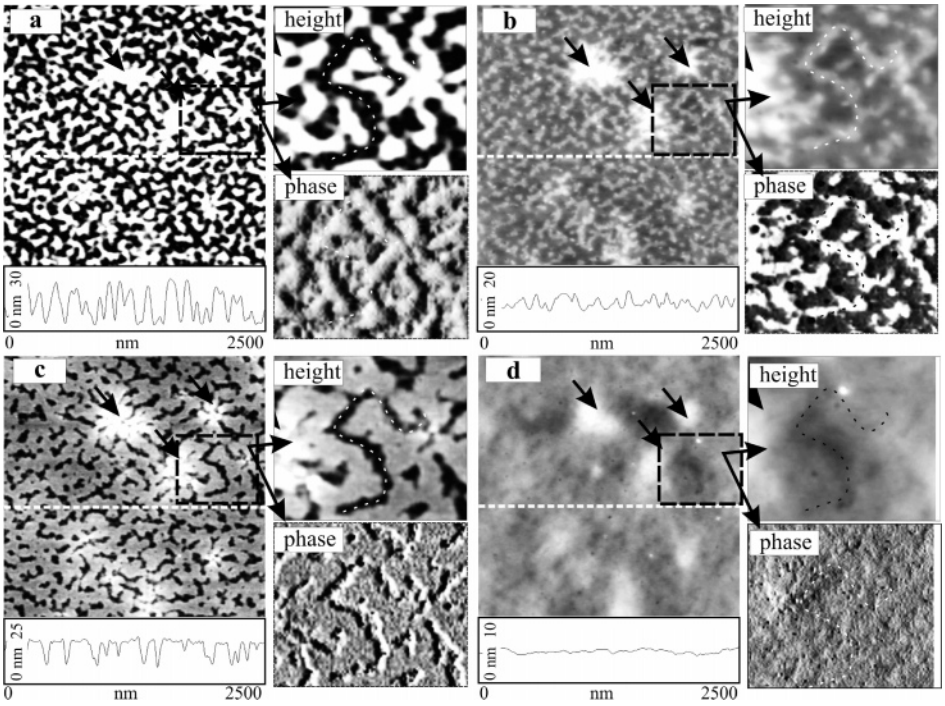

Figure 8. AFM height micrographs of the topography of brush IV after exposure to (a) acetone, (b) toluene, (c) acetic acid, and (d) dichloromethane. All micrographs were acquired from the same area, which can be identified with the help of three characteristic defects on the brush marked by arrows. The dashed black squares indicate areas magnifications (height and phase AFM images), which are shown on the right side of each original micrograph. The cross sections along the same place marked by dashed white lines are shown underneath the micrographs.

75 nm. The phase image (underneath the height image, on the right from Figure 8a) of the same area shows a two-component surface with a phase contrast of 30°. After treatment with acetic acid, which is a good solvent for PMMA, the Π pattern switched again back to a depression state (Figure 8c). The overall topography of the brush differs from that after treatment with acetone and exhibits a much smoother surface with trenchlike valleys inside, with a depth of 10 nm and a width of 50 nm. The roughness of the brush topography decreases by a factor of 2 (4 nm). The phase image, as after treatment with acetone, does not exhibit any significant variation in contrast, although here the Π pattern can be recognized in a more pronounced way.

After treating the brush with dichloromethane, which is a good solvent for both polymers, the topography switched, as expected, to a flat state with an rms roughness of only 0.6 nm (Figure 8d).

Conclusion

In this paper, we have discussed PS−PMMA mixed brushes with varying molecular weight and grafting densities. For all brushes the following observations hold: the solvent quality has a strong influence on the pattern formation. Exposure to acetone and acetic acid, which have a stronger interaction with the PMMA chains compared to PS, leads to preferential localization of PMMA chains on the topmost layer of the brush. Treatment with toluene, which is a good solvent for both polymers, results in a heterogeneous distribution of PS and PMMA chains on the surface of the brush, so that there are nanoscopic regions consisting only of PS or PMMA. Exposure to dichloromethane imposed a structure with flat, featureless topography with the PMMA chains preferentially adsorbed on the top. Size and shape of the formed pattern are also strongly influenced by the molecular parameters of the brushes. For example, when phase separation is induced through toluene treatment, the area of the brush surface occupied by the PMMA chains increases with the total amount of PMMA within a brush. The formed patterns persist over many cycles of topography switching, independent of brush structure or solvent used. The structure can be erased and regenerated over many cycles. However, if this is observed in more detail, slight differences between individual locations can be found. In an ensemble of the domains within the brush topography, there are patterns which appear at the same place with exactly the same shape each time after topography switching, while a certain part of the domains bear slight or strong variations in the position and shape over repeated treatment with different solvents. Such a process might be called partial domain memory, as some domain positions and shapes are exactly remembered, while this memory is more blurred in other locations.

In a forthcoming publication, we discuss how the domain memory effect can quantitatively be related to the molecular characteristics of the brush.

Acknowledgment. This work was supported by the Deutsche Forschungsgemeinschaft and the Landesstiftung Baden-Württemberg, Germany.

Supporting Information Available: AFM micrographs and movie of PS−PMMA brush II. This material is available free of charge via the Internet at http://pubs.acs.org.

References and Notes

(1) de Gennes, P. G. *Adv. Colloid Interface Sci.* **1987**, *27*, 189.
(2) Alexander, S. *J. Phys. (Paris)* **1977**, *38*, 983.
(3) Milner, S. T. *Europhys. Lett.* **1988**, *7*, 695.
(4) Zhulina, E. B.; Borisov, O. V.; Pryamitsyn, V. A.; Birshtein, T. M. *Macromolecules* **1991**, *24*, 140.
(5) Dong, H.; Marko, J. F.; Witten, T. A. *Macromolecules* **1994**, *27*, 6428.
(6) Milner, S. T.; Witten, T. A.; Cates, M. E. *Macromolecules* **1989**, *22*, 853.
(7) Matyjaszewski, K.; Patten, T. E.; Xia, J. H. *J. Am. Chem. Soc.* **1997**, *119*, 674.
(8) Zhao, B.; Brittain, W. J. *J. Am. Chem. Soc.* **1999**, *121*, 3557.

(9) Lemieux, M.; Usov, D.; Minko, S.; Stamm, M.; Shulha, H.; Tsukruk, V. V. *Macromolecules* **2003**, *36*, 7244.
(10) Motornov, M.; Minko, S.; Eichhorn, K.-J.; Nitschke, M.; Simon, F.; Stamm, M. *Langmuir* **2003**, *19*, 8077.
(11) Rühe, J.; Knoll, W. In *Supramolecular Polymers*; Ciferri, A., Ed.; Marcel Dekker: New York, 2000; pp 565−613.
(12) Zhao, B.; Brittain, W. J. *Prog. Polym. Sci.* **2000**, *25*, 677.
(13) Matyjaszewski, K.; Miller, P. J.; Shukla, N.; Immaraporn, B.; Gelman, A.; Luokala, B. B.; Siclovan, T. M.; Kickelbick, G.; Vallant, T.; Hoffmann, H.; Pakula, T. *Macromolecules* **1999**, *32*, 8716.
(14) Kong, X.; Kawai, T.; Abe, J.; Iyoda, T. *Macromolecules* **2001**, *34*, 1837.
(15) Kim, J. B.; Huang, W.; Bruening, M. L.; Baker, G. L. *Macromolecules* **2002**, *35*, 5410.
(16) Tomlinson, M. R.; Genzer, J. *Chem. Commun.* **2003**, 1350.
(17) Sidorenko, A.; Minko, S.; Schenk-Meuser, K.; Duschner, H.; Stamm, M. *Langmuir* **1999**, *15*, 8349.
(18) Kiriy, A.; Gorodyska, G.; Minko, S.; Jaeger, W.; Stepanek, P.; Stamm, M. *J. Am. Chem. Soc.* **2002**, *124*, 13454.
(19) Minko, S.; Patil, S.; Datsyuk, V.; Simon, F.; Eichhorm, K.; Motornov, M.; Usov, D.; Tokarev, I.; Stamm, M. *Langmuir* **2002**, *18*, 289.
(20) Zhao, B. *Langmuir* **2004**, *20*, 11748.
(21) LeMieux, M. C.; Julthongpiput, D.; Bergman, K. N.; Cuong, P. D.; Ahn, H.-S.; Lin, Y.-H.; Tsukruk, V. V. *Langmuir* **2004**, *20*, 10046.
(22) Feng, J.; Haasch, R. T.; Dyer, D. J. *Macromolecules* **2004**, *37*, 9525.
(23) Lin, Y.-H.; Teng, J.; Zubarev, E. R.; Shulha, H.; Tsukruk, V. V. *Nano Lett.* **2005**, *5*, 491.
(24) Minko, S.; Müller, M.; Usov, D.; Scholl, A.; Froeck, C.; Stamm, M. *Phys. Rev. Lett.* **2002**, *88*, 035502.
(25) Boyes, S. G.; Brittain, W. J.; Weng, X.; Cheng, S. Z. D. *Macromolecules* **2002**, *35*, 4960.
(26) Draper, J.; Luzinov, I.; Minko, S.; Tokarev, I.; Stamm, M. *Langmuir* **2004**, *20*, 4064.
(27) Prokhorova, S. A.; Kopyshev, A.; Ramakrishnan, A.; Zhang, H.; Rühe, J. *Nanotechnology* **2003**, *14*, 1098.
(28) Santer, S. A.; Rühe, J. *Polymer* **2004**, *45*, 8279.
(29) Marko, J. F.; Witten, T. A. *Phys. Rev. Lett.* **1991**, *66*, 1541.
(30) Singh, C.; Pickett, G. T.; Zhulina, E.; Balazs, A. C. *J. Phys. Chem. B* **1997**, *101*, 10614.
(31) Soga, K. G.; Zuckermann, M. J.; Guo, H. *Macromolecules* **1996**, *29*, 1998.
(32) Müller, M. *Phys. Rev. E* **2002**, *65*, 030802(R).
(33) Brown, G.; Chakrabarti, A.; Marko, J. F. *Europhys. Lett.* **1994**, *25*, 239.
(34) Goeffrey Soga, K.; Zuckermann, M. J.; Guo, H. *Macromolecules* **1996**, *29*, 1998.
(35) Boyes, S. G.; Granville, A. M.; Baum, M.; Akgun, B.; Mirous, B. K.; Brittain, W. J. *Surf. Sci.* **2004**, *570*, 1.
(36) Boyes, S. G.; Akgun, B.; Brittain, W. J.; Foster, M. D. *Macromolecules* **2003**, *36*, 9539.
(37) Zhao, B.; Brittain, W. J. *Macromolecules* **2000**, *33*, 8813.
(38) Zhao, B.; Brittain, W. J.; Zhou, W. S.; Cheng, S. Z. D. *Macromolecules* **2000**, *33*, 8821.
(39) Kwan, H.-Y.; Zhang, H.; Rühe J., manuscript in preparation.
(40) Prucker, O.; Rühe, J. *Macromolecules* **1998**, *31*, 592.
(41) Prucker, O.; Rühe, J. *Langmuir* **1998**, *14*, 6893.
(42) Prucker, O.; Rühe, J. *Macromolecules* **1998**, *31*, 602.
(43) Schimmel, M. PhD Dissertation, MPI for Polymer Research, Mainz, 1998.
(44) *Polymer Handbook*, 4th ed.; Brandrup, J., Immergut, E. H., Grulke, E. A., Eds.; John Wiley & Sons: New York, 1999.
(45) Magonov, S. N.; Elings, V.; Whangbo, M. H. *Surf. Sci. Lett.* **1997**, *375*, L385.
(46) Prokhorova, S. A.; Kopyshev, A.; Ramakrishnan, A.; Zhang, H.; Rühe, J. *Proc. SPIE, Nanotechnol.* **2003**, *5118*, 30.

MA060092Y